Sensitivity, Specificity, and the Hybridization Isotherms of DNA Chips

A. Halperin,* A. Buhot,* and E. B. Zhulina†
*Centre National de la Recherche Scientifique, Commissariat à l'Energie Atomique, Université Joseph Fourier, Grenoble, France and †Institute of Macromolecular Compounds of the Russian Academy of Sciences, St. Petersburg, Russia

ABSTRACT Competitive hybridization, at the surface and in the bulk, lowers the sensitivity of DNA chips. Competitive surface hybridization occurs when different targets can hybridize with the same probe. Competitive bulk hybridization takes place when the targets can hybridize with free complementary chains in the solution. The effects of competitive hybridization on the thermodynamically attainable performance of DNA chips are quantified in terms of the hybridization isotherms of the spots. These relate the equilibrium degree of the hybridization to the bulk composition. The hybridization isotherm emerges as a Langmuir isotherm modified for electrostatic interactions within the probe layer. The sensitivity of the assay in equilibrium is directly related to the slope of the isotherm. A simpler description is possible, in terms of c_{50} values specifying the bulk composition corresponding to 50% hybridization at the surface. The effects of competitive hybridization are important for the quantitative analysis of DNA chip results, especially when used to study point mutations.

INTRODUCTION

DNA microarrays allow us to interrogate the base sequence of DNA or RNA chains. They can be used to detect pathogens, identify genetic defects, monitor gene expression, etc. (Marshall and Hodgson, 1998; Gerhold et al., 1999; Graves, 1999; Niemeyer and Blohm, 1999; Southern et al., 1999; Wang, 2000; Pirrung, 2002). Despite the intense activity in this field, theoretical aspects of the function of DNA microarrays received relatively little attention. Early theoretical work focused on the dynamics of hybridization at the surface (Chan et al., 1995; Livshits and Mirzabekov, 1996). Recently, theoretical investigations considered the equilibrium hybridization isotherms of DNA chips (Vainrub and Pettitt, 2002, 2003) and polyelectrolyte aspects of the systems (Crozier and Stevens, 2003). In the following we present a theoretical analysis of the effect of competition between different possible hybridization reactions on the sensitivity and specificity of DNA chips. The discussion utilizes hybridization isotherms relating the equilibrium fraction of hybridized chains at the surface, x, to the composition of the bulk. The effects are revealed by comparison of the hybridization isotherms for competition-free situations with those obtained when competitive hybridization is significant. They are quantified in terms of various c_{50} values specifying the bulk composition corresponding to 50% hybridization at the surface. A key ingredient of our discussion is the derivation of the competition-free isotherm as a Langmuir adsorption isotherm modified to allow for electrostatic interactions. Our model is related to an earlier model proposed by Vainrub and Pettitt in that both assume uniform smearing of the electrical charge of the probe layer.

The elementary units of DNA microarrays are spots containing numerous single-stranded DNA (ssDNA) chains, of identical sequence, terminally anchored to the support surface. The spots are placed in a checkered pattern so that each sequence is allocated a unique site. These chains, or probes, preferentially hybridize with free ssDNA chains having a complementary sequence. The microarray is immersed in a solution containing labeled ssDNA chains whose sequence is not known and are commonly referred to as targets. The presence of specific sequences is signaled by hybridization on the corresponding spot as monitored by correlating the strength of the label signal with the position of the spot (Graves, 1999). Recently, label-free detection methods, involving optical and mass sensitive techniques, have attracted growing attention (Niemeyer and Blohm, 1999). These allow us to monitor the kinetics of hybridization. However, such methods measure the total hybridization of a particular probe irrespective of the identity of the partner. In marked contrast, selective labeling of a particular sequence monitors only the hybridization of this target and does not report on the hybridization of other moieties.

The unitization of DNA chips as analytical method involves immersing the device in a solution containing a mixture of DNA chains of different sequences and concentrations. Under such conditions, it is necessary to allow for the role of competitive hybridization. It is useful to distinguish between two types of competitive hybridization. Competitive surface hybridization occurs when a number of different targets can hybridize with the same probe. Thus, a site occupied by certain probes will preferentially hybridize DNA targets with a perfectly matched complementary sequence. However, it will also hybridize a certain fraction of mismatched sequences. As we shall discuss, this fraction depends on the binding constants as well as the concentrations of the moieties involved. Competitive hybridization at the surface clearly lowers both the sensitivity and the specificity of the assay. When the surface competition is significant, labeled and unlabeled detection may yield different results. No difference is expected when all targets are

Submitted June 5, 2003, and accepted for publication October 7, 2003.

Address reprint requests to Dr. Avraham S. Halperin, CNRS, SPrAM, DRFMC-SI3M/CEA-Grenoble, 17 rue des Martyrs, Grenoble 38054, France. Tel.: 33-47-644-0696; E-mail: ahalperin@cea.fr.

0006-3495/04/02/718/13 $2.00

labeled, as is the case when PCR amplification is used. On the other hand, when selective labeling of specific targets is possible, the two techniques measure different quantities corresponding to different isotherms. Competitive bulk hybridization reduces the concentration of nonhybridized targets that are available for hybridization with the probe. This takes place when the solution contains complementary sequences that can hybridize with the target in the solution. Such sequences may occur either in the same chain, leading to hairpin formation, or in different sequences leading to interchain hybridization. Competitive bulk hybridization diminishes thus the sensitivity of DNA chips. Its importance varies, again, with the binding constants and the concentrations. The issues discussed above assume their clearest form when DNA chips are used to identify single nucleotide polymorphism or point mutations (Lopez-Crapez et al., 2001). In these situations, the DNA chip is exposed to a mixture of targets differing from each other only in the identity of one particular base. The fraction of the different forms is then deduced from the relative intensity of the signals of the four spots corresponding to the four possible sequences.

In practice, the DNA chips are immersed in the target solution for a relatively short time. As a result, the attainment of equilibrium is not guaranteed and rates of the different hybridization reactions play an important role. Yet, full analysis of the reaction kinetics requires knowledge of the equilibrium state. An understanding of the equilibrium state is also necessary to identify the relative importance of kinetic and thermodynamic controls of the performance of the DNA microarrays. Finally, emerging evidence (Bhanot et al., 2003) suggests that the performance of DNA chips, as measured by the number of false-positives, is best at the thermodynamic equilibrium. With this in mind, we investigate the equilibrium hybridization isotherms for three idealized but experimentally attainable situations. These situations involve a DNA array immersed in solutions of different composition: 1), a solution containing one species of single-stranded target (Fig. 1); 2), a solution containing two different targets that do not hybridize in the bulk but are both capable of hybridizing with the same probe (Fig. 2); and 3), a solution containing two different chains—a target and a complementary chain capable of hybridizing with it in the bulk but incapable of hybridizing with the probe (Fig. 3). In all cases, we consider the case of probes and targets of equal length, i.e., that the number of bases, N, in the chains are identical. For brevity our discussion focuses on systems where the hybridization at the surface has a negligible effect on the concentration of targets in the bulk. This case corresponds to small spots or to elevated target concentration.

The first two sections summarize the necessary background information for the subsequent discussion. Thus, On Sensitivity and the Hybridization Isotherm recalls the definitions of sensitivity and other measures of the performance of analytical assays. The relationship between sensitivity and the equilibrium hybridization isotherm is also discussed. The structural characteristics of DNA chips and important length scales in the problem are summarized in Relevant Molecular Dimensions and Length Scales. The next section is devoted to the derivation of the competition-free hybridization isotherm as a Langmuir isotherm modified to allow for electrostatic interactions. Initially we obtain the hybridization isotherm for an arbitrary electrostatic free energy density of the probe layer, γ_{el}. We then consider the hybridization isotherms for particular functional forms of γ_{el} assuming a laterally uniform smearing of the electric charge. We mostly focus on the diffuse-layer model where the

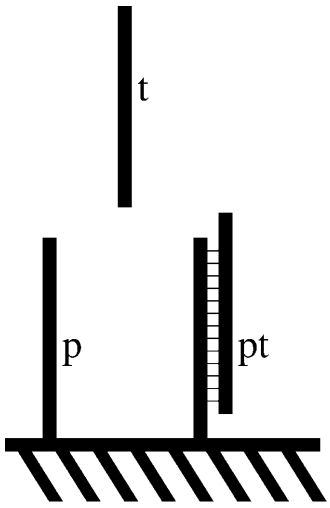

FIGURE 1 A schematic representation of the competition-free case where the probes, p, can hybridize with a single target species, t.

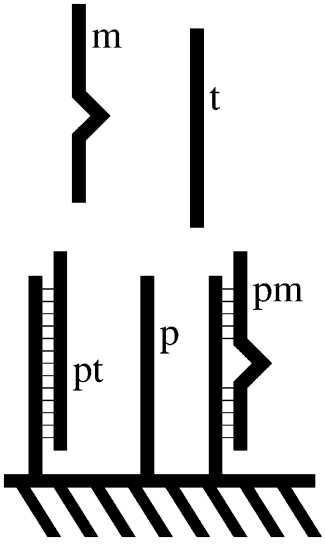

FIGURE 2 In the competitive surface hybridization case the probes, p, can hybridize with a perfectly matched target species, t, as well as with a mismatched target, m.

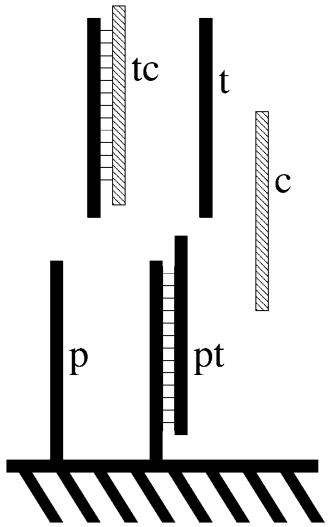

FIGURE 3 Competitive bulk hybridization when the probes, p, can hybridize with a single perfectly matched target species, t, but t can also hybridize in the bulk with a complementary chain, c; c cannot hybridize with p.

charge is uniformly smeared within the probe layer thus allowing for its thickness. It is important to note that some of our results are actually independent of the model specifying γ_{el}. We conclude this introductory section with a discussion of relevant experimental results and a comparison between our approach and the Vainrub-Pettitt (VP) model. In the remaining sections we pursue two complementary goals: the modifications of the hybridization isotherms to allow for competitive hybridization, and the resulting effects on the sensitivity and specificity of the assay. Three situations are considered. The competition-free case, when the probes are exposed to a single target, is discussed in Sensitivity, Selectivity, and C_{50} for Competition-Free Systems. This yields upper bounds for the sensitivity and the specificity. Competitive hybridization is analyzed in The Effect of Competitive Surface Hybridization and in The Effect of Competitive Bulk Hybridization. The detailed derivation of γ_{el} within the diffuse-layer model is described in Appendix A. The hybridization isotherm for low salt solutions is discussed in Appendix B.

ON SENSITIVITY AND THE HYBRIDIZATION ISOTHERM

As we shall see, the equilibrium hybridization isotherms naturally suggest characterization of the sensitivity of the assay in terms of appropriate c_{50} values. This characteristic is closely related to the common definitions of the sensitivity of analytical techniques. It is thus useful to first summarize these definitions and their relationship to the hybridization isotherms. Different definitions of sensitivity are available (Pardue, 1997, and references therein; Ekins and Edwards, 1997). The International Union of Pure and Applied Chemistry definition identifies the sensitivity, S_e, with the slope of the calibration curve. The calibration curve describes the measured response, R, to a target concentration, c_t, $R(c_t)$, and

$$S_e = dR/dc_t. \tag{1}$$

The quantitative resolution of the assay, Δc_t, is then specified by

$$\Delta c_t = \in_r (c_t)/S_e(c_t), \tag{2}$$

where $\in_r$ is the measurement error as given by its standard deviation. The detection limit, the lowest detectable c_t, is determined by $\Delta c_t(c_t = 0)$ since when the concentration c_t is lower than $\Delta c_t(c_t = 0)$, the error is larger than the signal. The International Federation of Clinical Chemistry and Laboratory Medicine convention identifies the sensitivity with the detection limit.

Our goal is to relate the sensitivity of DNA chips to their hybridization isotherms. With this in mind, it is convenient to adopt the IUPAC definition. This choice is motivated by the following observations: 1), the calibration curve in equilibrium is closely related to the hybridization isotherm; 2), the measurement error depends on the measurement technique and on instrumental characteristics. In distinction to $R(c_t)$, $\in_r$ is not related to the calibration curve; and 3), S_e as given by Eq. 1 plays a role in the determination of both the qualitative resolution and the detection limit.

In the following we will assume that $R(c_t)$ is proportional to the equilibrium hybridization fraction at the surface, x; i.e., $R(c_t) = \kappa x + const$ where κ is a constant. This assumption is justified when the following conditions are fulfilled: 1), nonspecific adsorption is negligible and R is due only to hybridization at the surface; 2), the duration of the experiment is sufficiently long to allow the hybridization to reach equilibrium; and 3), the measured signal depends linearly on the amount of oligonucleotides at the surface. It is useful to note the following points concerning the attainability of these conditions. First, surface treatments repressing nonspecific adsorption are available for certain substrates (Steel et al., 2000 and references therein). Second, the attainment of stationary state for the hybridization may require long periods of up to 14 h (Peterson et al., 2001, 2002; Bhanot et al., 2003). Furthermore, the degree of hybridization may depend on the thermal history (heating of the substrate or the solution). In this context it is important to stress that, by definition, a state of thermodynamic equilibrium is both stationary in time and independent of the path, i.e., preparation method. Finally, the linear range varies with the measurement technique. For example, when using fluorescent labels the linear regime occurs at low enough concentration when self-quenching is negligible (Lakowicz, 1999).

RELEVANT MOLECULAR DIMENSIONS AND LENGTH SCALES

Two groups of length scales play an important role in our subsequent discussion. One group describes the structural features of the probe layer. The second characterizes the electrostatic interactions and their screening. Expression of the free energies in terms of these length scales allows for a compact formulation and the identification of the relevant dimensionless variables.

The structural features of the layer are determined mostly by the dimensions of the hybridized and unhybridized probes as well as the grafting density (Graves, 1999; Southern et al., 1999; Pirrung, 2002). The number of monomers, nucleotides, per probe, N, varies over a wide range. Values of $10 \leq N \leq 30$ are common, but much higher values, of $N \approx 1000$, are attainable. In the following we will consider systems comprised of probes and targets of equal size in the range $10 \leq N \leq 30$. Double-stranded DNA (dsDNA) is a semiflexible chain with a persistence length $\approx 10^3$ Å (Cantor and Schimmell, 1980). Thus, in our N range double-stranded oligonucleotides may be viewed as rigid rods with the radius of a dsDNA, $r = 9.5$ Å, and a projected length per monomer along the axis of $2b = 3.4$ Å. The corresponding parameters for ssDNA are not yet established. Stacking interactions between the hydrophobic bases tend to produce a stiff ''single-stranded helix'' (Cantor and Schimmell, 1980; Bloomfield et al., 2000; and Korolev et al., 1998 and references therein). Since these interactions are noncooperative, this tendency is especially marked in short ssDNA considered by us. Theoretical studies of the melting behavior of free DNA in the bulk suggest that ssDNA can be modeled as a rigid rod with projected length per monomer of $a \approx 3.4$ Å and a radius of $r_{ss} \approx 7$ Å (Frank-Kamenetskii et al., 1987; Korolev et al., 1998). With this in mind we will approximate the length of single-stranded chains, Na, as identical to that of the double-stranded, $N2b$, denoting both by L. For $N = 30$ we thus have $L \approx 100$ Å.

The probes are chemically grafted to the surface via a short spacer chain. The attainable values of the area per probe, Σ, vary with the support surface (Graves, 1999; Southern et al., 1999; Pirrung, 2002). Typical values of Σ on glass surfaces are of order of 10^4 Å^2 corresponding to a distance $\Delta \approx 100$ Å between grafting sites. Significantly higher grafting densities of ssDNA are possible on polypropylene supports where Σ values of $\Sigma \approx 40$ Å^2, corresponding to $\Delta \approx 7$ Å, were reported. In this last case it is necessary to deplete the surface to allow full hybridization to take place. The mode of grafting can influence the orientation of the probe. Their orientation can also be affected by adsorption to the surface (Levicky et al., 1998). Thus ssDNA grafted onto untreated gold form a compact layer due to adsorption. The layer swells and extends into the solution after treatment with mercaptohexanol (Levicky et al., 1998). This treatment is also important for elimination of nonspecific adsorption of the targets. Our discussion assumes flexible junctions that enable free rotation and a nonadsorbing surface. Under these conditions, the average thickness of the probe layer, H, varies between $H \approx L/2$ at low grafting densities and $H \approx L$ when $\Sigma \ll L^2$.

Three electrostatic length scales are of importance to our discussion. One is the Bjerrum length, $l_B = e^2/\varepsilon kT$, where ε is the dielectric constant, k is the Boltzmann constant, and T is the temperature. In water, with $\varepsilon \approx 80$, $l_B \approx 7$ Å at room temperature. Note that the variation of ε with T contributes to the T dependence of l_B. The second is the Gouy-Chapman length $\Lambda = 1/2\pi l_B \sigma$. Here σ is the number of charges per unit area on a uniformly charged surface. Λ characterizes the spatial distribution of the counterions in the vicinity of a uniformly charged planar surface in a salt-free solvent. In this situation the majority of counterions are localized within a distance Λ from the surface. In the following the charge of the probes, hybridized or not, is assumed to be uniformly smeared. As a result, σ varies between N/Σ and $2N/\Sigma$, depending on x, the degree of hybridization. For an unhybridized layer, Λ is in the range of 10 to 10^2 Å. A third scale is the Debye length, r_D, characterizing the screening range of electrostatic interactions in a salt solution. For a 1:1 salt with number concentration of ions ϕ_s, it is $r_D = (8\pi l_B \phi_s)^{-1/2}$; thus, in a 1 M solution, $r_D = 3$ Å.

The range of DNA concentrations encountered in experiments varies between 10^{-6} M and 10^{-12} M. The solution usually also contains 1 M of 1:1 salt. Under these conditions the electrostatic interactions between the free targets are essentially fully screened.

THE COMPETITION-FREE HYBRIDIZATION ISOTHERM

The dependence of the hybridization degree, x, on the concentration of the target, c_t, is described by the hybridization isotherm. It is helpful to consider first an array of DNA probes of a single sequence, p, in contact with a solution containing a single species of ssDNA target, t. The hybridization of p and t creates a double-stranded oligonucleotide, pt, at the surface. For this choice of system the only reaction is $p + t \rightleftharpoons pt$ and no competitive hybridization reactions occur (Fig. 1). The factors determining the hybridization isotherm fall into two groups. One consists of the factors giving rise to the Langmuir isotherm (Evans and Wennerström, 1994), describing the adsorption of neutral adsorbates at a surface comprising a finite number of sites, each capable of accommodating a single adsorbate. These include: 1), the entropy of the free targets in solution; 2), the mixing entropy of the hybridized and unhybridized probes; and 3), the nonelectrostatic component of the hybridization free energy. The hybridization at the surface of a DNA chip differs from the Langmuir scenario in that both the adsorbates (the targets) and the surface (the probe layer)

are charged. As a result the free energies of the targets and the probe layer incorporate electrostatic terms. These allow for the electrostatic interaction energy between the charges and for the entropic effects associated with the polarization of the ionic clouds surrounding the macroions. In the following we will obtain a specific form for the electrostatic free energy of the probe layer by modeling it as a planar layer with a laterally uniform charge density. However, some of our conclusions are actually independent of the functional form of this term. With this in mind we introduce, at this point, an arbitrary electrostatic free energy per unit area, γ_{el}. The electric charge localized at the surface increases with the fraction of hybridized probes, x. Consequently, $\gamma_{el} = \gamma_{el}(x)$ increases with x, reflecting the growth of the electrostatic penalty with the hybridization degree. Initially we will obtain the hybridization isotherm in terms of this unspecified $\gamma_{el}(x)$. We will then consider the hybridization isotherms as obtained for two models for the charge distribution within the probe layer and the resulting explicit functional forms of $\gamma_{el}(x)$.

The equilibrium state of the hybridization reaction, $p+t \rightleftharpoons pt$, is determined by the condition, $\mu_{pt} = \mu_p + \mu_t$, where μ_i is the chemical potential of species i. Our discussion focuses on the case where the number concentration of the targets is only weakly diminished by this reaction, and is well approximated by the initial concentration, c_t. Since the target solution is dilute and the ionic strength of the solution is high, electrostatic interactions between the targets are screened. Consequently μ_t assumes the weak solution form of

$$\mu_t = \mu_t^0 + kT \ln c_t, \tag{3}$$

where μ_t^0 is the chemical potential of the reference state. Strictly speaking, $\mu_t = \mu_t^0 + kT \ln a_t$, where a_t is the activity (Moore, 1972). The dimensionless a_t is related to the concentration of t chain c_t via $a_t = \gamma c_t$, where γ is the activity coefficient. Since $\gamma \rightarrow 1$ as $c_t \rightarrow 0$ we will, for simplicity, express μ_t by Eq. 3, noting that c_t in this expression is dimensionless. When the concentration of targets is significantly modified by the hybridization with the probes, c_t should be replaced by $c_t' = c_t - xN_T/V$ where V is the volume of the solution and N_T the total number of probes. Such modification is necessary when c_t is very low or when the spots are large.

To obtain μ_{pt}, we first need to specify the free energy of the probe layer as a function of x. The N_T probes are immobilized at the surface, thus forming a two-dimensional grid of hybridization sites. At equilibrium, $N_{pt} = xN_T$ of the probes are hybridized, whereas $N_p = (1 - x)N_T$ remain unhybridized. The pt and p chains form thus a two-dimensional solution associated with a mixing entropy of $-kN_T[x \ln x + (1 - x)\ln(1 - x)]$. This two-dimensional solution is, however, nonideal because of the electrostatic interactions between the chains. Altogether, the free energy per probe site is

$$\gamma_{site} = \gamma_0 + x\mu_{pt}^0 + (1 - x)\mu_p^0 + \Sigma\gamma_{el} + kT[x \ln x + (1 - x)\ln(1 - x)], \tag{4}$$

where Σ is the area per probe and γ_0 is the free energy density of the bare surface of area Σ. μ_{pt}^0 and μ_p^0 are the chemical potentials of the p and pt states in a reference state to be discussed later. For simplicity we now limit the discussion to probes and targets with identical number of bases, N. Since each chain carries a charge of $-Ne$, the number charge density on a surface of total area A is $\sigma = N(N_p + 2N_{pt})/A = \sigma_0(1 + x)$, where $\sigma_0 = NN_T/A$ is the number charge density on the unhybridized surface and $\Sigma = A/N_T$.

It is convenient to reformulate the equilibrium condition, $\mu_{pt} = \mu_p + \mu_t$, in terms of the exchange chemical potential of the hybridized probe, $\mu_{pt}^{ex} = \mu_{pt} - \mu_p$. The exchange chemical potential of the hybridized probe is $\mu_{pt}^{ex} = \partial\gamma_{site}/\partial x$ or

$$\mu_{pt}^{ex} = \mu_{pt}^0 - \mu_p^0 + N\frac{\partial\gamma_{el}}{\partial\sigma} + kT \ln\frac{x}{1 - x}, \tag{5}$$

where $\Sigma(\partial\gamma_{el}/\partial x) = \Sigma(\partial\gamma_{el}/\partial\sigma)(\partial\sigma/\partial x) = N(\partial\gamma_{el}/\partial\sigma)$, since $\partial\sigma/\partial x = \sigma_0$ and $\Sigma\sigma_0 = N$. $N(\partial\gamma_{el}/\partial\sigma)$ is thus the electrostatic free energy penalty incurred upon hybridization for a given x. The equilibrium condition, $\mu_{pt}^{ex} = \mu_t$, then leads to the adsorption isotherm,

$$\frac{x}{c_t(1 - x)} = K_t \exp\left[-\frac{N}{kT}\frac{\partial\gamma_{el}}{\partial\sigma}\right], \tag{6}$$

where $K_t = \exp(-(\Delta G^0/kT))$ is the equilibrium constant for the hybridization reaction at the surface and $\Delta G^0 = \mu_{pt}^0 - \mu_p^0 - \mu_t^0$.

Our discussion up to this point did not involve a particular model for the charge distribution or a specific functional form of γ_{el}. In the remainder of this section we will consider the hybridization isotherm for particular forms of γ_{el} as obtained by assuming that the charges of the p and pt chains are uniformly smeared laterally. We will consider two models of this type. In the first the charges are distributed in an infinitely thin layer at the solid-liquid interface. This model ignores the structure of the probe layer and overestimates γ_{el}. It is, however, of interest as a simple model that captures the essential physics. The exact form of γ_{el} corresponding to this scenario, for the high salt regime encountered experimentally, is specified by the Poisson-Boltzmann (PB) equation for $r_D \ll \Lambda$ (Evans and Wennerström, 1994). This γ_{el} is identical to the one obtained by the use of the capacitor approximation. In this approximation γ_{el} is identified with the electrostatic energy of a planar capacitor, $2\pi(\sigma e)^2 d/\varepsilon$, with a charge density $\sigma = \sigma_0(1 + x)$ and a width $d = r_D$, thus leading to

$$\frac{\gamma_{el}}{kT} = 2\pi\sigma^2 l_B r_D. \tag{7}$$

For this choice of γ_{el} the hybridization isotherm Eq. 6 assumes the form

$$\frac{x}{c_t(1-x)} = K_t \exp[-\Gamma_c(1+x)], \tag{8}$$

where $(N/kT)(\partial\gamma_{el}/\partial\sigma) = \Gamma_c(1+x)$, and $\Gamma_c = 4\pi N\sigma_0 l_B r_D$ is the electrostatic free energy of a hybridized target in an unhybridized layer with a charge density σ_0.

The capacitor model accounts for the essential physics in a simple and transparent way. However, this model tends to overestimate the electrostatic free energy because all the charges of the DNA chains are placed on a surface. To avoid this problem we now assume instead that the charges are uniformly smeared within a layer of thickness H giving rise to a number charge density of $\rho = \sigma/H$. The analysis of this diffuse-layer model differs from that of the capacitor model only in the form of the electrostatic free energy density γ_{el}. To obtain γ_{el} we utilize a two-phase or box-approximation for the solution of the PB equation (Pincus, 1991; Wittmer and Joanny, 1993; Borisov et al., 1994). Within it, we distinguish between two regions: 1), a proximal region, adjacent to the charged surface, where the concentrations of ions deviates from the bulk values. The concentrations of each of the ionic species are constant and obey the Donnan equilibrium; and 2), a distal neutral region, where the effect of the charged surface is screened out and the concentrations of the ions are determined by the concentration of the salt. The ionic concentrations and the equilibrium electrostatic free energy are determined by minimization of the free energy with respect to the height of the proximal region. This approximation involves the simplest form of discretization of the PB equation. The details of the analysis are presented in Appendix A. In the following we focus on the experimentally relevant case of high salt such that $r_D \ll H$ and $r_D \ll (H\Lambda)^{1/2}$. The low salt regime is described in Appendix B. In the high salt regime the screening of the charged layer is dominated by the contribution of the salt and

$$\frac{\gamma_{el}}{kT} = 4\pi\sigma^2 l_B \frac{r_D^2}{H}. \tag{9}$$

The hybridization isotherm in this salt-screening (ss) regime is

$$\frac{x}{c_t(1-x)} = K_t \exp[-\Gamma(1+x)], \tag{10}$$

where $(N/kT)(\partial\gamma_{el}/\partial\sigma) \approx 8\pi N\sigma l_B(r_D^2/H) = \Gamma(1+x)$, and $\Gamma = 8\pi N\sigma_0 l_B(r_D^2/H)$ is the electrostatic penalty incurred by a *pt* chain in an unhybridized layer with $\sigma = \sigma_0$. Note that the functional form of Eq. 10 is identical to that of Eq. 8, but that $\Gamma = 2\Gamma_c r_D/H < \Gamma_c$.

As a reference state it is convenient to choose the state of a chain (ssDNA or dsDNA) anchored to a surface at a low grafting density such that the in-plane electrostatic interaction are negligible. When the lateral interactions are negligible, one may roughly approximate $\mu_{pt}^0(\mu_p^0)$ by the μ^0 of the corresponding free chain in the solution. This choice is useful in that it enables us to estimate the various hybridization constants using the nearest-neighbor parameter sets available in the literature (Bloomfield et al., 2000). It is, however, important to keep in mind the problems introduced by this choice of reference state and the approximation of $\mu_{pt}^0(\mu_p^0)$. One difficulty involves the electrostatic free energy. γ_{el} is obtained by the charging of a hypothetical noncharged layer. As a result, the electrostatic contribution to $\mu_{pt}^0(\mu_p^0)$ leads to a small overestimate of the electrostatic free energy. Note that for high σ or small Λ, fluctuation effects become important (Lau et al., 2002). These are not included in our analysis. In addition, caution is required in identifying the boundaries of the regime of negligible lateral interactions. This is because the decay of electrostatic interactions at an impenetrable surface is slower than in the bulk. Thus, point charges embedded at an impenetrable surface polarize a hemisphere of the ionic solution, thus giving rise to a dipole, and the lateral interactions decay as $1/r^3$ (Jancovici, 1982). Another problem concerns the rotational free energy of the chains. The rotational freedom of the terminally anchored chains is restricted by the impenetrable grafting surface. Further restrictions may be imposed by the grafting functionality. The diminished rotational freedom reduces the rotational term in the free energy per chain. This effect is, however, neglected when $\mu_{pt}^0(\mu_p^0)$ are approximated by μ^0 of the corresponding free chains. When both the target and probe are self-complementary it is necessary to allow for the change of symmetry due to the grafting. In turn, this requires an appropriate modification of $\mu_{pt}^0(\mu_p^0)$ with respect to their bulk counterparts. Finally, note that in the low grafting density regime, as discussed above, the hybridization isotherm is expected to assume the Langmuir form

$$\frac{x}{(1-x)c_t} = K_t. \tag{11}$$

In this regime the electrostatic aspect of the problem is evident only in the dependence of the μ^0 values, and thus K_t, on the concentration of salt.

The number of hybridization isotherms of DNA chips reported in the literature is rather small (Nelson et al., 2001; Peterson et al., 2001, 2002). The situation is further complicated because of paucity of data concerning N_T, the number of probes available to hybridization, and the related problem of ascertaining the attainment of thermodynamic equilibrium. The uniform smearing models for the hybridization isotherms are supported by two experimental studies carried out by the group of Georgiadis (Peterson et al., 2001, 2002). In one experiment the grafting density was varied in the range of $2 \times 10^{12} - 12 \times 10^{12}$ probes/cm^2 whereas c_t was kept constant at 1 μM (Peterson et al., 2001). A plot of $\ln[(1-x)/x]$ vs. $(1+x)/\Sigma$ can be fitted with a straight line with a slope smaller than the one predicted by the theory (Fig. 4). This is, however,

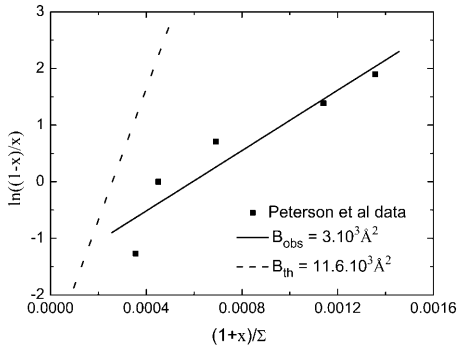

FIGURE 4 A plot of $\ln(1-x)/x$ vs. $(1+x)/\Sigma$ using the data of Peterson et al. (2002). Eq. 10 yields $\ln(1-x)/x = const' + B(1+x)/\Sigma$ with $B = 8\pi l_B N^2 r_D^2/H$. For the experiment cited $l_B = 7$ Å, $r_D = 3$ Å, $N = 25$, and $H = 85$ Å, leading to $B \simeq 1.16 \times 10^4$ Å^2 as compared to the observed $B \simeq 3 \times 10^3$ Å^2.

encouraging, inasmuch as the data was acquired in 1/2 h and is thus unlikely to reflect complete equilibrium. In the second group of experiments, the hybridization was studied for a lower grafting density of 1.5×10^{12} probes/cm^2, whereas c_t was varied over the range of 0 to 5 μM (Peterson et al., 2002). In this study the hybridization isotherm of the perfectly matched targets was well fitted by the Langmuir form. Importantly, this study established that the system failed to reach equilibrium without heating treatment for mismatched targets.

A hybridization isotherm of identical form to Eq. 8 and to Eq. 10 was announced earlier by Vainrub and Pettitt (2002, 2003). Vainrub and Pettitt also pointed out that some of the results of the Georgiadis group (Peterson et al., 2001, 2002) are consistent with this form. The VP approach is designed to permit the utilization of exact results on the interaction free energy between a penetrable charged sphere and an impenetrable charged surface in the strong screening regime when the Debye-Hückel approximation is applicable (Ohshima and Kondo, 1993). Within it, one calculates the excess free energy of a probe layer with xN_T hybridized probes, $F_{el}(x)$, with respect to the unhybridized layer. In effect, $F_{el}(x)$ is the sum of the contributions of xN_T hybridization events, $F_{el} = \sum_{i=1}^{xN_T} F_i(\sigma_i)$. Each step contributes $F_i(\sigma_i) = F_{pt}(\sigma_i) - F_p(\sigma_i)$, where $F_{pt}(F_p)$ is the electrostatic free energy of a *pt* (*p*) sphere in contact with a planar layer with charge density $\sigma_i = \sigma_0 + iN/A$. Thus, at each step the probe layer is modeled as a planar charged surface interacting with a single charged sphere. The steps differ in the charge density of the surface. The main difference between the VP approach and ours is in the handling of the charges. In the VP scheme some of the charges appear as charged spheres, whereas others appear as a charged surface. Within our model there is no duality and all charges are described in the same fashion. In practical terms, the VP approach cannot allow for the thickness of the probe layer nor can it be extended to describe hybridization at lower ionic strength.

SENSITIVITY, SELECTIVITY, AND C_{50} FOR COMPETITION-FREE SYSTEMS

The hybridization isotherms discussed in the two preceding sections describe DNA arrays in the absence of competitive hybridization in the bulk or at the surface. This situation is realized when an array comprised of a single type of probe is exposed to a solution of a single target. The concentration of target leading to 50% equilibrium hybridization in such systems, ${}^{t}c_{50}^{0} = K_t^{-1} \exp(N/kT(\partial\gamma_{el}/\partial\sigma)|_{x=1/2})$, is a useful characteristic of the system. Within the diffuse-layer model in the salt-screening (ss) regime, ${}^{t}c_{50}^{0}$ is

$$ {}^{t}c_{50}^{0} = \frac{1}{K_t}\exp\left(\frac{3}{2}\Gamma\right). \tag{12} $$

${}^{t}c_{50}^{0}$ is closely related to the sensitivity of the array,

$$ \begin{aligned} S_e(x) &= \frac{(1-x)^2}{1+x(1-x)\Gamma} K_t \exp[-\Gamma(1+x)] \\ &= \frac{(1-x)^2}{1+x(1-x)\Gamma} \frac{1}{{}^{t}c_{50}^{0}} \exp[-\Gamma(x-1/2)]. \end{aligned} \tag{13} $$

The sensitivity of the array, as defined by $S_e(x)$, varies with x and thus with c_t. It is maximal at $x = 0$ when

$$ S_e(0) = K_t \exp(-\Gamma) = \frac{1}{{}^{t}c_{50}^{0}} \exp\left(-\frac{\Gamma}{2}\right), \tag{14} $$

whereas at $x = 1/2$ it is $S_e(1/2) = 1/(4 + \Gamma){}^{t}c_{50}^{0}$. As we shall see, $S_e(0)$ is not affected by competitive hybridization. On the other hand, $S_e(x)$ and c_{50} are modified significantly by these processes.

Since $S_e(x) \sim 1/{}^{t}c_{50}^{0}$, clearly a lower ${}^{t}c_{50}^{0}$ is desirable and $1/{}^{t}c_{50}^{0}$ is a useful measure of the sensitivity of the array. Both $1/{}^{t}c_{50}^{0}$ and $S_e(x)$ decrease as Γ and the electrostatic penalty incurred by the hybridization increase. In the salt-screening regime, where most experiments are carried out, Γ increases with the grafting density as $\Gamma \sim \sigma_0$. Although higher sensitivity is expected at lower grafting densities, this does not ensure a lower detection limit or a better quantitative resolution. These last two parameters depend also on the measurement error, $\in_r$. In turn, $\in_r$ typically decreases as the grafting density, and the signal, increase. Thus, $1/{}^{t}c_{50}^{0}$ and $S_e(x)$ only provide partial guidance for the design of DNA arrays. Nevertheless, these two parameters do provide useful information regarding the performance of a DNA chip of a given design (that is, grafting density, grafting functionality, spot size, and detection method). Thus, the relative sensitivity of two different probe target pairs, p_1 t_1 and p_2 t_2, all other factors being equal, is

$$ \frac{{}^{t_1}S_e}{{}^{t_2}S_e} = \frac{{}^{t_2}c_{50}^{0}}{{}^{t_1}c_{50}^{0}} = \frac{K_{t_1}}{K_{t_2}}. \tag{15} $$

The specificity of a given probe, p, can be quantified by the

relative sensitivity when a p spot is exposed to a perfectly matched target, t, or to a mismatch, m,

$$\frac{{}^{t}S_e}{{}^{m}S_e} = \frac{{}^{m}c_{50}^{0}}{{}^{t}c_{50}^{0}} = \frac{K_t}{K_m}. \quad (16)$$

These two ratios also specify the corresponding ratios of the qualitative resolution and the detection limit. Importantly, Eqs. 15 and 16 are independent of the electrostatic penalty irrespective of the form of γ_{el}.

THE EFFECT OF COMPETITIVE SURFACE HYBRIDIZATION

The hybridization isotherm requires modification when the bulk solution contains more than one ssDNA species capable of hybridization at the surface. In this situation the different species compete for hybridization with the probes. For simplicity we consider the case of a binary solution comprising a target (t) and a mismatched ssDNA (m) with a concentration c_m and a standard chemical potential in the bulk solution μ_m^0. It is placed in contact with a single component probe layer such that the p chains are perfect matches to the targets (Fig. 2). We further assume that the m and t chains are of the same length. The number of probes that hybridized with m is $N_m = yN_T$. In this case, $\sigma = N(N_p + 2N_{pt} + 2N_{pm})/A = \sigma_0(1 + x + y)$ and

$$\gamma_{site} = \gamma_0 + x\mu_{pt}^0 + y\mu_{pm}^0 + (1 - x - y)\mu_p^0 + \Sigma\gamma_{el} + kT[x\ln x + y\ln y + (1 - x - y)\ln(1 - x - y)], \quad (17)$$

where μ_{pm}^0 is the standard chemical potential of a hybridized pm at the surface. In this situation, the hybridization isotherm is determined by two equilibrium conditions, $\mu_{pt}^{ex} = \mu_t$ (as before), and $\mu_{pm}^{ex} = \mu_m$. In obtaining the explicit form of these conditions, note that $(\partial\Sigma\gamma_{el}/\partial x) = (\partial\Sigma\gamma_{el}/\partial y) = N(\partial\gamma_{el}/\partial\sigma)$ because $(\partial\sigma/\partial x) = (\partial\sigma/\partial y) = \sigma_0$. The exchange chemical potentials of the hybridized m and t are thus given by

$$\mu_{pt}^{ex} = \mu_{pt}^0 - \mu_p^0 + N\frac{\partial\gamma_{el}}{\partial\sigma} + kT\ln\frac{x}{1 - x - y}, \quad (18)$$

$$\mu_{pm}^{ex} = \mu_{pm}^0 - \mu_p^0 + N\frac{\partial\gamma_{el}}{\partial\sigma} + kT\ln\frac{y}{1 - x - y}, \quad (19)$$

and the chemical potential of the free m is

$$\mu_m = \mu_m^0 + kT\ln c_m. \quad (20)$$

As before, we focus on the small-spot limit where the bulk concentrations of m and t are not affected by the hybridization at the surface. The hybridization behavior of this system is described by three isotherms specifying the hybridization degrees of t and m individually as well as the total hybridization:

$$\frac{x}{c_t(1 - x - y)} = K_t\exp\left[-\frac{N}{kT}\frac{\partial\gamma_{el}}{\partial\sigma}\right], \quad (21)$$

$$\frac{y}{c_m(1 - x - y)} = K_m\exp\left[-\frac{N}{kT}\frac{\partial\gamma_{el}}{\partial\sigma}\right], \quad (22)$$

$$\frac{x + y}{(1 - x - y)} = (c_mK_m + c_tK_t)\exp\left[-\frac{N}{kT}\frac{\partial\gamma_{el}}{\partial\sigma}\right], \quad (23)$$

where $K_t = \exp(-(\Delta G^0/kT))$, $K_m = \exp(-(\Delta G_m^0/kT))$, and $\Delta G_m^0 = \mu_{pm}^0 - \mu_p^0 - \mu_m^0$. The observed isotherm depends on the method used to interrogate the surface. Thus, utilization of selectively tagged t will reveal Eq. 21; use of selectively tagged m will show Eq. 22; and detection methods sensitive to overall hybridization mass, such as surface plasmon resonance, will yield Eq. 23. The explicit form of the hybridization isotherms within the diffuse model in the salt-screening regime is obtained by substituting $N/kT(\partial\gamma_{el}/\partial\sigma) = \Gamma(1 + x + y)$. Note that K_t, K_m, and Γ can be determined from experiments involving exposure of the DNA chip to single component solutions of t and m chains.

The specificity of the assay can be quantified by considering the fraction of incorrectly hybridized probes, P_m. Equations 21 and 22 yield $y = x(c_m/c_t)(K_m/K_t)$ and thus

$$P_m = \frac{y}{x + y} = \frac{c_mK_m}{c_mK_m + c_tK_t}. \quad (24)$$

Within this definition the specificity strongly depends on c_m, or to be precise, on $(c_m/c_t)(K_m/K_t)$. The fraction of mismatched probes is small, $P_m \ll 1$, so long as $c_m \ll c_t(K_m/K_t)$. At $c_m = c_t(K_m/K_t)$, one-half of the hybridized probes are mismatched, $P_m = 1/2$; whereas for $c_m \gg c_t(K_m/K_t)$, P_m approaches unity. Equation 24 is independent of the electrostatic contribution irrespective of the form of γ_{el}. It is also useful to consider the ratio of ${}^{t}c_{50}^{0}$ to c_{50}, the bulk concentration of t giving rise to 50% pt hybridization in the presence of a mismatch of concentration c_m. In contrast to P_m, the expression for ${}^{t}c_{50}^{0}/{}^{t}c_{50}$ does depend on γ_{el}. For the diffuse-layer model in the salt-screening regime, it is given by

$$\frac{{}^{t}c_{50}^{0}}{{}^{t}c_{50}} = \left(1 - \frac{c_m}{{}^{m}c_{50}^{0}}\frac{{}^{t}c_{50}^{0}}{{}^{t}c_{50}}\right)\exp\left(-\frac{\Gamma}{2}\frac{c_m}{{}^{m}c_{50}^{0}}\frac{{}^{t}c_{50}^{0}}{{}^{t}c_{50}}\right). \quad (25)$$

In the low grafting density regime, when $\Gamma = 0$, Eq. 25 assumes the form $({}^{t}c_{50}/{}^{t}c_{50}^{0}) = 1 + (c_m/{}^{m}c_{50}^{0})$. In all cases, ${}^{t}c_{50} = {}^{t}c_{50}^{0}$ when $c_m = 0$, and ${}^{t}c_{50} > {}^{t}c_{50}^{0}$ for $c_m > 0$. In other words, the sensitivity, as measured by $1/{}^{t}c_{50}$, decreases as c_m increases (Fig. 5).

THE EFFECT OF COMPETITIVE BULK HYBRIDIZATION

A different type of competition occurs when the targets can hybridize in the bulk as well as at the surface. Such competition can arise in three different situations: 1), The solution contains targets as well as complementary strands, c. These can be perfectly matched or mismatched sequences.

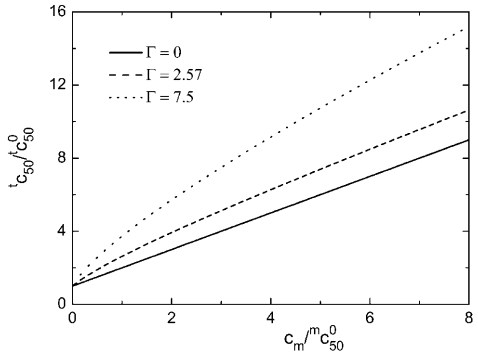

FIGURE 5 Plots of $^{t}c_{50}/^{t}c_{50}^{0}$ vs. $c_m/^{m}c_{50}^{0}$, as given by Eq. 25, for the case of competitive surface hybridization involving a probe, p, of the sequence CAACTTGATATTAATA, a target, t, GTTGAACTATAATTAT, and a mismatched target, m, GTTGA*G*CTATAATTAT (TG mismatch). In the three cases depicted, $T = 300°K$, $N = 16$, $H = 54$ Å, $l_B = 7$ Å, and $r_D = 3$ Å. The continuous line corresponds to the low grafting density regime where $\Gamma = 0$. The two others are $\Sigma = H^2 = 2916$ Å^2 leading to $\Gamma = 2.57$ (*dashes*), and $\Sigma = 10^3$ Å^2 leading to $\Gamma = 7.5$ (*dots*). The standard Gibbs free energies per mole at 37°C are $\Delta G_t^0 = 12.4$ kcal/mole and $\Delta G_m^0 = 10.1$ kcal/mole (Tibanyenda et al., 1984). Since the ΔG^0 are per mole rather than per molecule, the equilibrium constants at $T = 300°$K, neglecting the T dependence of the ΔG^0, are $K_t = \exp(-\Delta G_t^0/RT) \simeq 10^{9.0}$ and $K_m = \exp(\Delta G_m^0/RT) \simeq 10^{7.4}$, where R is the gas constant. The corresponding $^{t}c_{50}^{0}$ values are 10^{-9} M, $10^{-7.4}$ M, and $10^{-4.1}$ M, respectively. The values of $^{m}c_{50}^{0}$ are $10^{-7.4}$ M, $10^{-5.7}$ M, and $10^{-2.5}$ M.

The c chains hybridize with the targets to form free double-stranded tc DNA chains. Thus, the $t+c \rightleftharpoons tc$ reaction in the bulk competes with the $t+p \rightleftharpoons pt$ reaction at the surface (Fig. 3). 2), The targets are self-complementary, and thus capable of undergoing a bulk hybridization reaction $t+t \rightleftharpoons tt$ in addition to $t+p \rightleftharpoons pt$, where p now denotes the immobilized t probe. 3), A third possible scenario involves formation of hairpins.

As explained in Relevant Molecular Dimensions and Length Scales, within our discussion the lengths of the p and pt chains are identical. Accordingly we will focus on the first two cases where the length of the chains does not change upon hybridization. Initially, we discuss the $t+c \rightleftharpoons tc$ scenario and then comment on the modification required to adapt the analysis to the $t+t \rightleftharpoons tt$ case. Again, we focus on the small-spot limit assuming that the hybridization with the probes has a negligible effect on the concentration of the targets. The hybridization isotherm describing this situation, for the two cases of interest, is

$$\frac{x}{(1-x)[t]} = K_t \exp\left[-\frac{N}{kT}\frac{\partial \gamma_{el}}{\partial \sigma}\right] \tag{26}$$

and $N/kT(\partial\gamma_{el}/\partial\sigma) = \Gamma(1+x)$ in the ss-regime of the diffuse-layer model. Importantly, the hybridization isotherm is modified in that c_t, the total concentration of t, is replaced by the equilibrium t concentration, $[t]$. In turn, $[t]$ is determined by the mass action law governing the bulk hybridization reaction. The combination of Eq. 26 with the appropriate mass action law is equivalent to the equilibrium condition specified by $\mu_t + \mu_p = \mu_{pt}$ and $\mu_t + \mu_c = \mu_{tc}$.

In the $t+c \rightleftharpoons tc$ scenario the mass action law is $[tc]/[t][c] = K$, where $[i]$ is the equilibrium concentration of species i, and K is the equilibrium constant of the bulk hybridization reaction for the temperature and ionic strength considered. This is supplemented by the mass conservations relations $[t] + [tc] = c_t$ and $[c] + [tc] = c_c$, where c_i denotes the total concentration of i. $[t]$ is then specified by

$$K[t]^2 + \{K(c_c - c_t) + 1\}[t] - c_t = 0. \tag{27}$$

When the hybridization with the probes has a significant effect on the concentration of the targets, $[t] + [tc] = c_t$ should be replaced by $[t] + [tc] + xN_T/V = c_t$. For brevity, we will not consider this case. It is instructive to analyze the effect of the competitive bulk hybridization for a number of simple situations. When the equilibrium favors the reactants, $[t] \approx c_t$ and the hybridization isotherm retains the competition-free form, Eq. 6. Such is the case in the presence of large excess of t, $c_t \gg c_c$, or when K is sufficiently small, i.e., $c_c \gg c_t$ or $c_c \approx c_t$ but $Kc_c \ll 1$. Significant modification of the hybridization isotherm occurs when the bulk hybridization equilibrium favors the products. This situation occurs in two simple cases: when $Kc_c \gg 1$ with either $c_c \gg c_t$ or $c_c \approx c_t$. We initially discuss briefly the first situation when

$$[t] \approx \frac{c_t}{Kc_c} \ll c_t, \tag{28}$$

leading to

$$\frac{x}{(1-x)} = \frac{c_t}{Kc_c} K_t \exp\left[-\frac{N}{kT}\frac{\partial \gamma_{el}}{\partial \sigma}\right]. \tag{29}$$

To obtain an explicit form of the isotherm within the ss-regime of the diffuse-layer model we substitute $\Gamma(1+x)$ for $N/kT(\partial\gamma_{el}/\partial\sigma)$. However, the effect on $^{t}c_{50}$ is independent of the model. In comparison to $^{t}c_{50}^{0} = K_t^{-1} \exp(N/kT(\partial\gamma_{el}/\partial\sigma)|_{x=1/2})$, $^{t}c_{50}$ increases to

$$^{t}c_{50} = Kc_c\, ^{t}c_{50}^{0} \gg ^{t}c_{50}^{0}. \tag{30}$$

The sensitivity, as measured by $1/^{t}c_{50}$, is thus reduced by a factor of $Kc_c \gg 1$. When $c_c \approx c_t$ and $Kc_c \gg 1$, the equilibrium condition (Eq. 27) yields

$$[t] \approx \left(\frac{c_t}{K}\right)^{1/2}, \tag{31}$$

thus leading to

$$\frac{x}{(1-x)} = \left(\frac{c_t}{K}\right)^{1/2} K_t \exp\left[-\frac{N}{kT}\frac{\partial \gamma_{el}}{\partial \sigma}\right]. \tag{32}$$

The corresponding $^{t}c_{50}$ increases thus to

$$^{t}c_{50} = K(^{t}c_{50}^{0})^2, \tag{33}$$

and the sensitivity, as measured by $1/^{t}c_{50}$, is reduced by a factor of $K^{t}c_{50}^{0} \gg 1$ in comparison to the competition-free

scenario. The sensitivity $S_e = dx/dc_t$ does depend on the form of γ_{el}. When Eq. 33 is applicable, S_e, as specified by the uniform density model at the ss-regime, is

$$S_e = \frac{K_t^2}{2K}\exp[-2\Gamma(1+x)]\frac{(1-x)^3}{x[1+\Gamma x(1-x)]} = \frac{1}{2^t c_{50}}\exp[-\Gamma(2x-1)]\frac{(1-x)^3}{x[1+\Gamma x(1-x)]}. \quad (34)$$

However, in the limit of $c_t \to 0$, the effect of the competitive bulk hybridization is negligible and $S_e(0)$ is thus given by Eq. 14. This is also the case for the $c_c \gg c_t$ and $Kc_c \gg 1$ scenarios considered earlier.

In the low grafting density regime, when γ_{el} is independent of σ, the hybridization isotherm for $c_c \approx c_t$ with $Kc_c \gg 1$ assumes the form $x/(1-x) = K_t(c_t/K)^{1/2}$. Upon defining $K_{eff} = K_t^2/K$ this isotherm can be expressed as

$$x = \frac{(K_{eff}c_t)^{1/2}}{1+(K_{eff}c_t)^{1/2}}. \quad (35)$$

This form is of interest because it resembles the isotherm obtained from the Sips model (Sips, 1948). The Sips model provides a generalization of the Langmuir isotherm in which the single binding energy, utilized in the Langmuir version, is replaced by a distribution of binding energies thus leading to an expression of the form

$$x = \frac{(K_{eff}c_t)^a}{1+(K_{eff}c_t)^a}, \quad (36)$$

where a is a characteristic of the distribution function. Thus, competitive bulk hybridization can give rise to a Sips isotherm with $a = 1/2$, even though the underlying mechanism is completely different. This is of interest, because the Sips isotherm was recently reported to allow for improved fitting of hybridization data (Peterson et al., 2002).

When the competitive bulk hybridization involves self-complementary chains, $t+t \rightleftharpoons tt$, the preceding discussion requires modification. In this case the mass action law assumes the form $[tt]/[t]^2 = K$ and the corresponding mass conservation relation becomes $[t] + 2[tt] = c_t$. $[t]$ is thus determined by $2K[t]^2+[t]-c_t = 0$. When $Kc_t \ll 1$ the competitive effect is negligible and $[t] \approx c_t$. In the opposite limit, $Kc_t \gg 1$, the bulk hybridization is important and $[t] \approx (c_t/2K)^{1/2}$. The $t+t \rightleftharpoons tt$ scenario thus closely resembles the $t+c \rightleftharpoons tc$ case when $c_t \approx c_c$. Note, however, that care must be taken in estimating K_t for the self-complementary case. When the sequences of the p and t chains are identical, K_t differs from the bulk K because the grafting to the surface modifies the symmetry of the chain (in addition to the factors discussed in The Competition-Free Hybridization Isotherm).

DISCUSSION

The hybridization isotherms of DNA chips provide a natural starting point for the analysis of their sensitivity and specificity. Clearly, this description is incomplete in that it is limited to equilibrium states, whereas in typical experiments equilibrium is not attained. The hybridization isotherms are nevertheless of interest because of the emerging evidence that the best performance of DNA chips is obtained in thermodynamic equilibrium (Bhanot et al., 2003). Accordingly, the selectivity and specificity obtained from the hybridization isotherms provide upper bounds to the performance of these assays. This approach is also of interest because an understanding of the equilibrium state is a prerequisite for the full analysis of the kinetics of hybridization. When selectivity is discussed in terms of the slope of the response curve, it is necessary to use an explicit form of the hybridization isotherm. We obtained such an explicit expression by use of the diffuse-layer model. In this model the charges of the pt and p chains are uniformly smeared within the probe layer. However, the analysis of the hybridization isotherm also suggests the use of various c_{50} values as measures of the specificity and selectivity of DNA chips. This description affords an important advantage in that the effects of competitive hybridization can be described in a form that is independent of the model used to specify the electrostatic interactions. Thus, the best performance of DNA chips is attained in competition-free situations used to define ${}^t c_{50}^0$, ${}^m c_{50}^0$, etc. One can then analyze the effects of competitive hybridization in terms of the increase in ${}^t c_{50}$ in comparison to ${}^t c_{50}^0$. This analysis also indicates that the knowledge of the competition-free isotherms allows us to predict the isotherms realized when competitive hybridization occurs. In addition the observed isotherm depends on the measurement technique when competitive surface hybridization is important, i.e., label-free detection differs from the detection of selectively labeled targets.

Much of our discussion concerns the effects of competitive hybridization. In certain applications the effects of competitive surface hybridization can be minimized by proper design of the probes (Lockhart et al., 1996; Li and Stormo, 2001; Bhanot et al., 2003). Such is the case, for example, when studying the expression level of genes of known sequence. However, this strategy cannot be employed when DNA chips are used to identify single nucleotide polymorphism or point mutations. Probe design is also of limited value in counteracting the effects of competitive bulk hybridization.

The results we obtained are based on the equilibrium hybridization isotherms. They are formulated in terms of the equilibrium fractions x, y, etc. of hybridized probes. In confronting these predictions with experimental results it is important to note the following two points. First, to specify x and y, it is necessary to first determine the number of probes available to hybridization, N_T. Thus it is not sufficient to ascertain the number of p chains immobilized at the surface. It is also necessary to confirm that this corresponds to the number of hybridized probes at equilibrium with a large excess of targets. This brings us to the second point

concerning the equilibrium state. This plays a role both in the determination of N_T, as discussed above, and in the determination of equilibrium fractions of hybridized probes. Here we recall again that a stationary state does not necessarily imply equilibrium. An equilibrium state should also be independent of the preparation method or sample history. In the context of DNA chips it is thus important to verify that the stationary state is not affected by a heating treatment. In every case, the equilibration time can be very long with periods of up to 14 h reported in the literature. It is also useful to note that the equilibration time depends on the bulk composition, c_t and c_m, on the ionic strength, and the grafting density, Σ. It also varies with the number of mismatches and their identity. Accordingly, the equilibration time in one experimental situation is not necessarily identical to the equilibration time under different conditions. When studying simultaneously the hybridization on different spots the equilibration rates for the different spots may well differ.

It is useful to distinguish between two types of experiments involving DNA chips: experiments designed to elucidate the physical chemistry of their function, and experiments utilizing DNA chips to analyze biological samples. In the first category, the experimental setup allows for selective labeling and for precise control of the composition of the bulk solution. It is straightforward to confront our analysis with such physical chemistry experiments. The situation with respect to analytical applications is more complex. Analytical experiments typically rely on PCR amplification of biological samples. As a result, selective labeling is impossible and the composition of the bulk solution is determined by the composition of the original sample and the amplification scheme, i.e., the choice of primers. Our discussion reveals difficulties in the quantitative interpretation of the results of such experiments, especially when used to study point mutations. In this last situation, one may quantify errors introduced by the competitive hybridization by use of standard addition—i.e., study a series of solutions obtained from the amplified biological sample by addition of different amounts of synthetic, selectively labeled target. The practical importance of these difficulties and the methods to overcome them remain to be established.

APPENDIX A: THE BOX MODEL FOR A DIFFUSE AND FOR A PLANAR LAYER

We consider a diffuse layer carrying Q charges distributed uniformly in a region of height H such that the total charge is $-Qe < 0$. The resulting number charge density is $\rho = Q/AH = \sigma/H$, where $\sigma = Q/A$ is the corresponding surface number density of charges and A is total surface area. In the limit of $H = 0$ this system reduces to the case of a charged surface. The analytical solution of the PB equation for this last case is known. Accordingly we will also investigate the box model for the $H = 0$ to demonstrate that it recovers the known results up to a numerical factor.

The surface charge affects the distribution of ions within a proximal layer of height, $\lambda > H$, adjacent to the surface. Within this layer $n_\pm$ is the total number of univalent positive (negative) ions and $\phi_\pm = n_\pm/\lambda A$ are the corresponding number concentrations. The electrical potential in the box, Ψ, determines the deviation of $\phi_\pm$ from the bulk number concentration ϕ_s via $\phi_\pm = \phi_s \exp(\mp e\Psi/kT)$, thus leading to the Donnan equilibrium,

$$\phi_+ \phi_- = \phi_s^2. \tag{37}$$

The overall electroneutrality of the proximal layer, $n_+ - n_- = Q$ leads to

$$\Delta\phi = \phi_+ - \phi_- = \sigma/\lambda. \tag{38}$$

λ is the neutralization length of the system, in that the net charge of a thicker layer is zero, and at higher altitude $\Psi = 0$. Combining Eqs. 37 and 38 leads to a quadratic equation, $\phi_+^2 - (\sigma/\lambda)\phi_+ - \phi_s = 0$, determining $\phi_\pm$. Upon introducing the parameters $s = r_D/\Lambda$ and $x = \lambda/\Lambda$, we obtain

$$\phi_\pm = \phi_s \left[\pm \frac{2s^2}{x} + \left(1 + \frac{4s^4}{x^2}\right)^{1/2} \right]. \tag{39}$$

The excess entropy of the ions in the box, with respect to the bulk, is specified by $-S/k = n_- \ln(\phi_-/\phi_s) + n_+ \ln(\phi_+/\phi_s)$. Invoking Eqs. 37 and 38 leads to $-S/k = A\sigma \ln(\phi_+/\phi_s)$, and the excess entropy per unit area is thus

$$-\frac{S}{Ak} = \sigma \ln \left[\frac{2s^2}{x} + \left(1 + \frac{4s^4}{x^2}\right)^{1/2} \right]. \tag{40}$$

The charge per unit area that is bound by a surface of height z is $ez(-\rho + \Delta\phi)$ when $0 \le z \le H$ and $e(-\rho + z\Delta\phi)$ when $H \le z \le \lambda$ (Fig. 6). Consequently, the electrostatic field, $E(z)$, as determined by the Gauss theorem, is

$$E(z) = \begin{cases} E_{in}(z) = \dfrac{4\pi e\sigma}{\varepsilon}\left(-\dfrac{1}{H} + \dfrac{1}{\lambda}\right)z & 0 \le z \le H \\ E_{out}(z) = \dfrac{4\pi e\sigma}{\varepsilon}\left(-1 + \dfrac{z}{\lambda}\right) & H \le z \le \lambda \end{cases}. \tag{41}$$

In the $H = 0$ case the charge per unit area below z is $e(-\rho + z\Delta\phi)$ and $E(z) = E_{out}(z)$ for $0 \le z \le \lambda$. The associated electrostatic energy per unit area, $W = \varepsilon/8\pi \int_0^\lambda E^2(z)dz$, is

$$\frac{W}{kT} = \frac{\sigma x}{3}\left(1 - \frac{H}{x\Lambda}\right)^2. \tag{42}$$

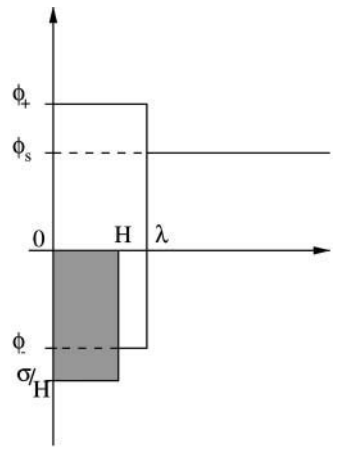

FIGURE 6 The concentration profiles of ions within the box model for the diffuse layer. The uniformly smeared charge of the p and pt chains is depicted by the shaded step function. It causes the concentration of negative and positive ions, ϕ_- and ϕ_+, within the proximal layer of thickness, λ, to deviate from the bulk value, ϕ_s.

In the case of $H = 0$ this reduces to $\sigma x/3$. Altogether, the electrostatic free energy per unit area is

$$\frac{\gamma_{el}}{kT} = \frac{\sigma x}{3}\left(1 - \frac{H}{x\Lambda}\right)^2 + \sigma \ln\left[\frac{2s^2}{x} + \left(1 + \frac{4s^4}{x^2}\right)^{1/2}\right]. \quad (43)$$

The equilibrium condition $\partial\gamma_{el}/\partial x = 0$ leads to

$$x^2\left(1 + \frac{4s^4}{x^2}\right)^{1/2}\left[1 - \left(\frac{H}{x\Lambda}\right)^2\right] = 6s^2. \quad (44)$$

We first consider the $H = 0$ case when

$$x^2\left(1 + \frac{4s^4}{x^2}\right)^{1/2} = 6s^2. \quad (45)$$

In the high salt limit, when $s \ll 1$, this leads to equilibrium values of $x \approx 6^{1/2}\, s$ and $\gamma_{el}/kT \approx 2(2/3)^{1/2}\sigma s \approx 1.6\,\sigma s$ or

$$\lambda \approx 6^{1/2} r_D \quad \gamma_{el}/kT \approx 4\pi(2/3)^{1/2}\sigma^2 l_B r_D, \quad (46)$$

as compared to $\gamma_{el}/kT = \sigma s$ obtained from the rigorous solution of the PB equation. In the opposite limit, of $s \gg 1$, corresponding to low salt, Eq. 45 leads to $x \approx 3$ and $\gamma_{el}/kT \approx 2\sigma[\ln 2s + (1 - \ln 3)/2]$ or

$$\lambda \approx 3\Lambda \quad \gamma_{el}/kT \approx 2\sigma \ln(4\pi\sigma l_B r_D), \quad (47)$$

whereas the rigorous solution of the PB equation is $\gamma_{el}/kT \approx 2\sigma[\ln 2s - 1]$. Thus, the box model for the planar layer recovers the rigorous solutions of the PB equation up to numerical corrections. In the low salt regime it yields the correct leading term $\gamma_{el}/kT \approx 2\sigma \ln s$. However, at high salt the box model overestimates γ_{el} by 60%. This performance is indicative of the errors expected from the model for the diffuse layer.

When $H > 0$, the equilibrium condition Eq. 44 is applicable. This equation differs from Eq. 45 in two respects: 1), a $[1 - (H/x\Lambda)^2]$ factor arising from the modification of the charge distribution and the associated electrostatic energy and 2), the problem now contains an additional length scale, H. We expect that $\lambda \gtrsim$ H, and consequently the magnitude of $4s^4/x^2 = 4r_D^4/\lambda^2\Lambda^2$ can be large (small) even when $s = r_D/\Lambda \ll 1$ ($s \gg 1$), provided $H \ll r_D$ ($H \gg r_D$). To allow for this last feature it is convenient to express Eq. 44 in terms of $y = \lambda/H$ instead of x, leading to

$$(y^2 - 1)\left[1 + \frac{4s^4}{y^2}\left(\frac{\Lambda}{H}\right)^2\right]^{1/2} = 6s^2\left(\frac{\Lambda}{H}\right)^2. \quad (48)$$

In analyzing the asymptotic solutions of this equation it is useful to compare the neutralization length, λ, with H. Two principle regimes emerge. When $\lambda \gg H$ ($y \gg 1$), the structure of the diffuse layer is irrelevant and we recover the solutions of the PB equation describing a charged planar layer. In this PB limit, Eq. 48 reduces to $y^2[1+(4s^4/y^2)(\Lambda/H)^2]^{1/2} = 6s^2(\Lambda/H)^2$. Here we can again distinguish between two regimes. When $s^2\Lambda/yH \gg 1$ this leads to $y \approx 3\ \Lambda/H \gg 1$, whereas for $s^2\Lambda/yH \ll 1$ we obtain $y \approx 6^{1/2}\, s\Lambda/H$. Altogether,

$$\lambda \approx \begin{cases} 3\Lambda & H \ll \Lambda \text{ and } r_D \gg \Lambda \\ 6^{1/2} r_D & H \ll r_D \text{ and } r_D \ll \Lambda \end{cases}. \quad (49)$$

When $\lambda \approx \Lambda$ the screening of the electrostatic potential is due to the counterions of the charged layer. The coions, originating from the salt, dominate the screening when $\lambda \approx r_D$. The crossover between the salt-screening (PBss) and counterions-screening (PBcs) regimes in the PB limit occurs at $s^2\Lambda/yH = 1$, leading to $s = 1$ or $\Lambda = r_D$.

When $y \gtrsim 1$ the charge distribution within the diffuse layer plays an important role. In this case it is useful to express y as $y = 1 + \delta$ and to solve with respect to $\delta \ll 1$. Eq. 44 reduces to $2\,\delta[1 + (2\,s^2\Lambda/H)^2]^{1/2} = 6\,s^2\Lambda^2/H^2$. Consequently we can distinguish between two cases depending on the magnitude of $s^2\Lambda/H$. When $s^2\Lambda/H \gg 1$ or $r_D^2 \gg \Lambda H$, we obtain $\delta \approx 3\Lambda/2H$. In the opposite limit, of $s^2\Lambda/H \ll 1$ or $r_D^2 \ll \Lambda H$, we obtain $\delta \approx 3\,(\Lambda/H)^2 s^2$. That is,

$$\lambda \approx \begin{cases} H + \frac{3}{2}\Lambda & H \gg \Lambda \quad \text{and} \quad r_D^2 \gg \Lambda H \\ H + 3\frac{r_D^2}{H} & H \gg r_D \quad \text{and} \quad r_D^2 \ll \Lambda H \end{cases}. \quad (50)$$

When $\lambda \approx H + 3\Lambda/2$ the screening is due to the counterions, whereas for $\lambda \approx H + 3r_D^2/H$ it is dominated by the coions. The crossover between the salt-screening (ss) and counterions-screening (cs) regimes is specified by $s^2\Lambda/H = 1$ or $\Lambda = r_D^2/H$. Additional crossover clearly occurs at $r_D = H$ and at $\Lambda = H$ (Fig. 7).

To obtain the corresponding asymptotic expressions for γ_{el}, it is convenient to rewrite Eq. 43 in terms of y as

$$\frac{\gamma_{el}}{kT} = \sigma\left\{\frac{H}{3\Lambda}\frac{(y-1)^2}{y} + \ln\left[\frac{2s^2\Lambda}{yH} + \left(1 + \left(\frac{2s^2\Lambda}{yH}\right)^2\right)^{1/2}\right]\right\}. \quad (51)$$

When $\Lambda/H \ll 1$ and $s^2\Lambda/H \gg 1$ (cs-regime), $y \approx 1 + 3\Lambda/2H$, the logarithmic term is dominant, and $\gamma_{el}/kT \approx \sigma \ln(4s^2\Lambda/H)$. In the limit of $r_D/H \ll 1$ and $s^2\Lambda/H \ll 1$ (ss-regime), when $y \approx 1 + 3r_D^2/H^2$, the logarithmic term can be expanded in powers of $s^2\Lambda/H$ leading to $\gamma_{el}/kT \approx 2\sigma r_D^2/H\Lambda$. When $\Lambda/H \gg 1$ and $s^2\Lambda/H \gg 1$ (PBcs regime), the logarithmic term is dominant and $\gamma_{el}/kT \approx \sigma[1+\ln(4s^2/3)]$, whereas for $r_D/H \gg 1$ and $s^2\Lambda/yH \ll 1$ (PBss regime), the logarithm can be expanded, leading to $\gamma_{el}/kT \approx 2(2/3)^{1/2}\,\sigma r_D/\Lambda$. The four scaling regimes are summarized in Table 1.

APPENDIX B: THE HYBRIDIZATION ISOTHERM AT LOW SALT

A novel form of the hybridization isotherm is obtained at low salt, when the screening is dominated by the counterions of the p and pt chains. This is the

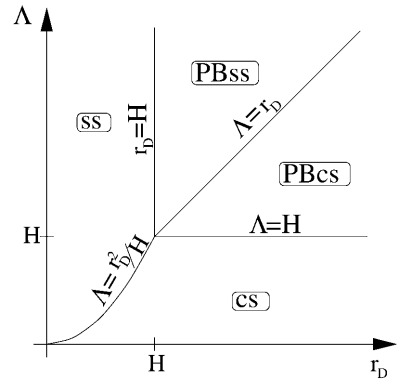

FIGURE 7 The asymptotic regimes of the diffuse layer within the box model. In the two PB regimes (PBcs and PBss), the neutralization length, λ, is large, $\lambda \gg H$, and the layer behaves as a charged planar surface. In the two remaining regimes, $\lambda \gtrsim H$ and the charge distribution of the layer, ρ, plays a role. In the cs-regions, the screening is dominated by the counterions, whereas in the ss-regions it is due to coions originating from the salt.

TABLE 1

Regime	γ_{el}/kT	λ	Range
cs	$\sigma \ln(\sigma l_B r_D^2/H)$	$H + 3\Lambda/2$	$\Lambda < H$ and $r_D > (\Lambda H)^{1/2}$
ss	$\sigma^2 l_B r_D^2/H$	$H + 3r_D^2/H$	$r_D < H$ and $r_D < (\Lambda H)^{1/2}$
PBcs	$\sigma \ln(\sigma l_B r_D)$	3Λ	$\Lambda > H$ and $r_D > \Lambda$
PBss	$\sigma^2 l_B r_D$	$6^{1/2} r_D$	$r_D > H$ and $r_D < \Lambda$

case when the concentration of counterions within the probe layer is much larger than the concentration of coions contributed by the salt, leading to $r_D > (\Lambda H)^{1/2}$ and $\Lambda \ll H$. In this situation,

$$\frac{\gamma_{el}}{kT} = \sigma \ln\left(8\pi\sigma l_B \frac{r_D^2}{H}\right). \quad (52)$$

The hybridization isotherm in this cs-regime is

$$\frac{x}{c_t(1-x)} = K_t \exp[-\Gamma_{cs} - N\ln(1+x)], \quad (53)$$

where $N/kT(\partial\gamma_{el}/\partial\sigma) \approx \Gamma_{cs} + N\ln(1+x)$ and $\Gamma_{cs} = N[\ln(8\pi\sigma_0 l_B (r_D^2/H)) + 1]$. The cs-regime is of interest in that it provides an additional test for the diffuse-layer model.

The authors benefited from instructive discussions with T. Livache and P. Pincus.

E.B.Z. was funded by the Centre National de la Recherche Scientifique and the Université Joseph Fourier.

REFERENCES

Bhanot, G., Y. Louzoun, J. Zhu, and C. DeLisi. 2003. The importance of thermodynamic equilibrium for high throughput gene expression arrays. *Biophys. J.* 84:124–135.

Bloomfield, V. A., D. M. Crothers, and I. Tinoco. 2000. Nucleic Acids: Structures, Properties and Functions. University Science Books, Sausalito, CA.

Borisov, O. V., E. B. Zhulina, and T. M. Birshtein. 1994. Diagram of the states of a grafted polyelectrolyte layer. *Macromolecules*. 27:4795–4803.

Cantor, C. R., and D. M. Schimmell. 1980. Biophysical Chemistry. WH Freeman, New York.

Chan, V., D. J. Graves, and S. McKenzie. 1995. The biophysics of DNA hybridization with immobilized oligonucleotide probes. *Biophys. J.* 69: 2243–2255.

Crozier, P. S., and M. J. Stevens. 2003. Simulations of single grafted polyelectrolytes chains: ssDNA and dsDNA. *J. Chem. Phys.* 118:3855–3860.

Ekins, R., and P. Edwards. 1997. On the meaning of ''sensitivity.'' *Clin. Chem.* 43:1824–1830.

Evans, D. F., and H. Wennerström. 1994. The Colloid Domain. VCH, New York.

Frank-Kamenetskii, M. D., V. V. Anshelevich, and A. V. Lukashin. 1987. Polyelectrolyte model of DNA. *Sov. Phys. Usp.* 30:317–330.

Gerhold, D., T. Rushmore, and T. Caskey. 1999. DNA chips: promising toys have become powerful tools. *TIBS*. 24:168–173.

Graves, D. J. 1999. Powerful tools for genetic analysis come of age. *Trends Biotechnol.* 17:127–134.

Jancovici, B. 1982. Classical Coulomb systems near a plane wall. I. *J. Stat. Phys.* 28:43–65.

Korolev, N., A. P. Lyubartsev, and L. Nordenskiöld. 1998. Application of polyelectrolyte theories for analysis of DNA melting in the presence of Na^+ and Mg^{2+} ions. *Biophys. J.* 75:3041–3056.

Lakowicz, J. R. 1999. Principles of Fluorescence Spectroscopy. Kluwer Academic/Plenum Press, New York.

Lau, A. W. C., D. B. Lukatsky, P. Pincus, and S. A. Safran. 2002. Charge fluctuations and counterion condensation. *Phys. Rev. E.* 65:051502.

Levicky, R. T. M., T. M. Herne, M. J. Tarlov, and S. K. Satija. 1998. Using self-assembly to control the structure of DNA monolayers on gold: a neutron reflectivity study. *J. Am. Chem. Soc.* 120:9787–9792.

Li, F., and G. D. Stormo. 2001. Selection of optimal DNA oligos for gene expression arrays. *Bioinformatics*. 17:1067–1076.

Livshits, M. A., and A. D. Mirzabekov. 1996. Theoretical analysis of the kinetics of DNA hybridization with gel-immobilized oligonucleotides. *Biophys. J.* 71:2795–2801.

Lockhart, D. J., H. Dong, M. C. Byrne, M. T. Follettie, M. V. Gallo, M. S. Chee, M. Mittmann, C. Wang, M. Kobayashi, H. Horton, and E. L. Brown. 1996. Expression monitoring by hybridization to the high-density oligonucleotide arrays. *Nat. Biotechnol.* 14:1675–1680.

Lopez-Crapez, E., T. Livache, J. Marchand, and J. Grenier. 2001. K-ras mutation detection by hybridization to a polypyrrole DNA chip. *Clin. Chem.* 47:186–194.

Marshall, A., and J. Hodgson. 1998. DNA chips: an array of possibilities. *Nat. Biotechnol.* 16:27–31.

Moore, W. J. 1972. Physical Chemistry. Longman, London, UK.

Nelson, B. P., T. E. Grimsrud, M. R. Liles, R. M. Goodman, and R. M. Corn. 2001. Surface plasmon resonance imaging measurements of DNA and RNA hybridization adsorption onto DNA microarrays. *Anal. Chem.* 73:1–7.

Niemeyer, C. M., and D. Blohm. 1999. DNA microarrays. *Angew. Chem. Int. Ed.* 38:2865–2869.

Ohshima, H., and T. Kondo. 1993. Electrostatic interactions of an ion penetrable sphere with a hard plate: contribution of image charges. *J. Coll. Interf. Sci.* 157:504–508.

Pardue, H. L. 1997. The inseparable triangle: analytical sensitivity, measurement uncertainty and quantitative resolution. *Clin. Chem.* 43: 1831–1837.

Peterson, A. W., R. J. Heaton, and R. M. Georgiadis. 2001. The effect of surface probe density on DNA hybridization. *Nucleic Acids Res.* 29: 5163–5168.

Peterson, A. W., L. K. Wolf, and R. M. Georgiadis. 2002. Hybridization of mismatched and partially matched DNA at surfaces. *J. Am. Chem. Soc.* 124:14601–14607.

Pincus, P. 1991. Colloid stabilization with grafted polyelectrolytes. *Macromolecules*. 24:2912–2919.

Pirrung, M. C. 2002. How to make a DNA chip. *Angew. Chem. Int. Ed.* 41:1277–1289.

Sips, R. 1948. On the structure of a catalyst surface. *J. Chem. Phys.* 16:490–495.

Southern, E., K. Mir, and M. Shchepinov. 1999. Molecular interactions on microarrays. *Nat. Genet.* 21:5–9.

Steel, A. B., R. L. Levicky, T. M. Herne, and M. J. Tralov. 2000. Immobilization of nucleic acids at solid surfaces: effect of oligonucleotide length on layer assembly. *Biophys. J.* 79:975–981.

Tibanyenda, N., S. H. De Bruin, C. A. Haasnoot, G. A. van der Marel, J. H. van Boom, and C. W. Hilbers. 1984. The effect of single base-pair mismatches on the duplex stability of d(T-A-T-T-A-A-T-A-T-C-A-A-G-T-T-G)·d(C-A-A-C-T-T-G-A-T-A-T-T-A-A-T-A). *Eur. J. Biochem.* 139: 19–27.

Vainrub, A., and M. B. Pettitt. 2002. Coulomb blockage of hybridization in two-dimensional DNA arrays. *Phys. Rev. E.* 66:041905.

Vainrub, A., and M. B. Pettitt. 2003. Surface electrostatic effects in oligonucleotide microarrays: control and optimization of binding thermodynamics. *Biopolymers*. 68:265–270.

Wang, J. 2000. From DNA biosensors to gene chips. *Nucleic Acids Res.* 28:3011–3016.

Wittmer, J., and J. F. Joanny. 1993. Charged diblock copolymers at interfaces. *Macromolecules*. 26:2691–2697.